Calculation of the Binding Energy of Nuclear Matter by the Method of Reference Spectrum*

M. RAZAVY†
Laboratory of Nuclear Studies, Cornell University, Ithaca, New York
(Received 7 November 1962)

The binding energy of nuclear matter has been calculated with the Hamada-Johnson potential by the method of the reference spectrum of Bethe *et al.* Corrections due to the exclusion principle, difference of spectrums, and the motion of the center of mass have not been included, these are believed to be small. It is found that the binding energy is only -7.8 MeV per particle at a density corresponding to the Fermi momentum $k_F=1.12\text{F}^{-1}$. This result is similar to the result of the calculations by Brueckner and Masterson with the Breit potential. A discussion of the self-consistency of the method is given.

I. INTRODUCTION

THE recent work of Bethe *et al.*[1] provides a simple and accurate method, "the reference spectrum," to investigate properties of nuclear matter. Details of theory and its application to a simple potential are given in their paper. The three-body clusters have been studied within the framework of this method by Rajaraman. These two papers together form a complete basis for an accurate numerical work with a realistic two-body potential. During the past year two sets of such potentials have been proposed by Hamada and Johnson[2] and by Breit *et al.*[3] In this paper we apply the method of the reference spectrum to calculate the binding energy of nuclear matter using the Hamada-Johnson potential for the nucleon-nucleon interaction. While this is an extensive numerical work, it is by no means complete. We have neglected the exclusion principle and spectral corrections to the reference spectrum which according to the estimates by BBP[4] is about 6% of the potential energy. We have not accounted for the motion of the center of mass. Altogether this may change our result by one or two MeV from an exact calculation, but this hardly affects the main features of our result, viz., that the binding energy is only about one-half of the accepted value and the equilibrium spacing is large compared to the experimentally observed one. These calculations were first done for $k_F=1.5$ F^{-1} with reference spectrum parameters $m^*=0.8$ and $\Delta=0.75$ (Sec. IV). However, the self-consistency requirement on the result of the first calculation suggested the use of a larger m^* and a smaller Δ, so we repeated the computation using $m^*(k_F)=1-0.1(k_F/1.5)^3$ and $\Delta=0.6$, for $k_F=1.1$, 1.3, and 1.5 F^{-1}.

In Sec. II we present a method to find the modified Moszkowski-Scott separation distance and to calculate the short and long range parts of the reaction matrix. We use this method to separate ^1S and ^3S waves only, where the separation seems to be an important improvement over the integration of the complete reaction matrix in reducing the corrections due to the exclusion principle. In Sec. III, we calculate the diagonal elements of the reaction matrix for the reference spectrum for S, P, and D waves. The effect of higher partial waves have been accounted for by using the Born approximation which is valid for these waves. In Sec. IV, we find the single-particle energies and the binding energy per particle, and we also investigate the problem of self-consistency. In the last section, Sec. V, we compare the results of this calculation with the work of Brueckner and Masterson[5] and discuss the lack of agreement with experimental observations.

II. THE SEPARATION METHOD

The fundamental equation of the reference spectrum method for the lth partial wave is[6]

$$\left[\frac{d^2}{dr^2}-\frac{l(l+1)}{r^2}-\gamma^2-m^*v\right]\chi_l=-m^*v\varphi_l, \qquad (2.1)$$

where $\chi_l=\varphi_l-r\psi_l$ is the difference between the free particle wave function $\varphi_l=rj_l(k_0r)$ and the perturbed wave function $r\psi_l(k_0r)$. γ^2 is a constant related to Δ by[7]

$$\gamma^2=2\Delta k_F^2-k_0^2 \quad \text{if} \quad k_0<k_F,$$
$$\gamma^2=3(\Delta k_F^2+k_0^2)-0.6k_F^2 \quad \text{if} \quad k_0>k_F,$$

m^* and Δ being the parameters of the reference spectrum. The matrix element of G^R, the reaction matrix for the reference spectrum is given by[8]

$$\langle k_0|G^R|k_0\rangle=4\pi\int_0^\infty \varphi_l(k_0r)vr\psi_l(k_0r)dr$$
$$=4\pi\frac{(\gamma^2+k_0^2)\hbar^2}{m^*M}\int_0^\infty \varphi_l(k_0r)\chi_l(k_0r)dr. \qquad (2.2)$$

* Supported in part by the joint program of the office of Naval Research and the U. S. Atomic Energy Commission.
† Present address: Theoretical Physics Institute, University of Alberta, Edmonton, Canada.
[1] (a) H. A. Bethe, B. H. Brandow, and A. G. Petschek, Phys. Rev. **129**, 225 (1963); and (b) R. Rajaraman, *ibid.* **129**, 265 (1963). The first of these references will be designated BBP in the text.
[2] T. Hamada and I. D. Johnson, Nucl. Phys. **34**, 383 (1962).
[3] K. E. Lassila, M. H. Hull, Jr., H. M. Ruppel, F. A. McDonald, and G. Breit, Phys. Rev. **126**, 881 (1962).
[4] Reference1 (a) Sec. 9.—This estimate is for the Gammel-Thaler potential.
[5] K. A. Brueckner and K. S. Masterson, Jr., Phys. Rev. **128**, 2267 (1962).
[6] See reference 1(a), Eq. (5.11).
[7] See reference 1(a), Eqs. (7.7) and (7.14).
[8] See reference 1(a), Eqs. (5.1) and (5.2).

The last integral can be divided into two parts

$$\int_0^\infty = \int_0^c + \int_c^\infty .$$

For $r<c$, $\chi_l(k_0r)=\varphi_l(k_0r)$, the true wave function being zero inside the core. The first part is a simple integral of spherical Bessel functions:

$$\int_0^c r^2 j_l^2(k_0r)dr = \frac{1}{2k_0^2}\left[c-\frac{\sin 2k_0c}{2k_0}\right] \quad \text{if} \quad l=0,$$

$$= \tfrac{1}{2}c^3[j_l^2(k_0c)-j_{l-1}(k_0c)j_{l+1}(k_0c)]$$

otherwise.

At $r=c$,

$$\chi_l(k_0c)=\varphi_l(k_0c) \tag{2.3}$$

is the boundary condition for the differential Eq. (2.1). The other boundary condition is at infinity

$$\chi_l(\infty)=0. \tag{2.4}$$

For S waves (2.1) reduces to

$$[(d^2/dr^2)-\gamma^2-m^*v]\chi=-m^*v\varphi. \tag{2.5}$$

Now, we follow the method of Moszkowski and Scott and separate the potential into a short- and a long-range part. The separation distance d is a point where the wave function in the reference spectrum joins smoothly to the unperturbed wave function. Since χ and χ' are continuous functions of r, it follows that[9]

$$\chi(d)=0 \tag{2.6a}$$

and

$$\chi'(d)=0. \tag{2.6b}$$

We have three boundary conditions (2.3), (2.6a), and (2.6b) to satisfy; this is possible since d is an arbitrary parameter. To find out the necessary conditions on the other parameters of (2.5) for the existence of a non-trivial d (since $v\to 0$ as $r\to\infty$, $d=\infty$ is always a solution), and to solve for χ, we factorize (2.5) into three first-order differential equations[10]:

$$dY_1/dr=-[1+f(r)Y_1^2], \tag{2.7}$$

$$dY_2/dr=-Y_1[f(r)Y_2+m^*v\varphi], \tag{2.8}$$

$$dY_3/dr=f(r)[Y_3Y_1+Y_2]+m^*v\varphi, \tag{2.9}$$

where $f(r)=-(\gamma^2+m^*v)$. The first two equations are subject to the following boundary conditions:

$$Y_1(c)=0 \tag{2.10a}$$

and

$$Y_2(c)=\varphi(c). \tag{2.10b}$$

The two equations (2.7) and (2.8) must be integrated outwards, which can be done without difficulty since Y_1 is negative and the second equation has an asymptotic behavior like a negative exponential. The point where $Y_2(r)$ is zero is the desired point d

$$Y_2(d)=0. \tag{2.11}$$

At this point we put

$$Y_3(d)=0 \tag{2.12}$$

and integrate (2.9) inwards to c. This is also easy since Y_3 behaves as an increasing exponential. $\chi(r)$ and $\chi'(r)$ are then given by

$$\chi(r)=Y_3(r)Y_1(r)+Y_2(r), \tag{2.13}$$

$$\chi'(r)=-Y_3(r), \tag{2.14}$$

as can be verified by direct substitution in Eqs. (2.7)–(2.9). From (2.11) and (2.12) it follows that, at $r=d$, $\chi(d)=\chi'(d)=0$, and at $r=c$, $\chi(c)=Y_2(c)=\varphi(c)$.

The condition for the existence of the point d can be seen by solving Eq. (2.8) subject to the boundary condition (2.10b):

$$Y_2(r)=\exp\left[-\int_c^r Y_1f(r)dr\right]$$

$$\times\left\{\varphi(c)-\int_c^r m^*v\varphi Y_1\exp\left[\int^r Y_1f(r)dr\right]dr\right\}. \tag{2.15}$$

Since $Y_2(c)=\varphi(c)>0$, if we show that for large values of r

$$\varphi(c)-\int_c^r m^*v\varphi Y_1\exp\left[\int^r Y_1fdr\right]dr<0, \tag{2.16}$$

then $Y_2(r)$ has a root for $r=d$. The following approximation makes it simpler to see the behavior of the left side of (2.16) as r increases. In the range $c<r<\infty$ the average value of v (denoted by $\bar{v}$) is much smaller than γ^2, so that in (2.7) we can neglect v compared to γ^2 which makes it possible to integrate it

$$Y_1(r)=-(1/\gamma)\tanh\gamma(r-c). \tag{2.17}$$

Substituting in (2.16) for Y_1 and f, we obtain

$$\varphi(c)+\int_c^r \frac{m^*}{\gamma}v\varphi\sinh\gamma(r-c)dr<0. \tag{2.18}$$

For practical values of γ, $\sinh\gamma(r-c)$ increases much faster than v decreases, and the integrand is negative ($v<0$); therefore, the integral increases without limit as r increases, so for some value of r the inequality (2.18) holds. Moreover, if the sign of φ remains the same over a sufficiently wide range of r, then the point d where $Y_2(r)$ changes sign can be within this range. Thus a finite separation distance exists if the potential on the average is attractive, if $\gamma^2\gg|m^*\bar{v}|$ and if the relative momentum k_0 is small enough so that φ is not oscillating over the range of interest, $c<r<d$.

[9] See reference 1(a), Sec. 10; also S. A. Moszkowski and B. L. Scott, Ann. Phys. (N.Y.) **11**, 65 (1960).

[10] E. C. Ridley, Proc. Cambridge Phil. Soc. **53**, 442 (1957).

TABLE I. The separation distance, the short- and long-range parts, and the complete reaction matrix for ^1S state are given as functions of relative momentum k_0; $k_F=1.5$ F^{-1}.

k_0/k_F	0	$(0.1)^{1/2}$	$(0.2)^{1/2}$	$(0.3)^{1/2}$	$(0.6)^{1/2}$
$d(k_0)$ (F)	1.076	1.088	1.107	1.127	1.198
W^s (MeV)	16.5	16.5	16.4	16.4	16.3
W^l (MeV)	−71.2	−48.	−36.5	−29.	−8.4
W^s+W^l (MeV)	−54.7	−31.5	−20.1	−12.6	7.9
W^R (MeV)	−59.2	−34.2	−21.2	−12.2	7.9

The results of the integration of the differential equations (2.7), (2.8), and (2.9) together with Eq. (2.13) enables us to find the matrix elements of G^s and v^l;

$$\langle k_0|G^s|k_0\rangle=4\pi\frac{(\gamma^2+k_0^2)\hbar^2}{m^*M}\int_0^d\frac{\sin k_0r}{k_0}\chi(k_0r)dr, \quad (2.19)$$

$$\langle k_0|v^l|k_0\rangle=4\pi\int_d^\infty\frac{\sin^2k_0r}{k_0^2}v(r)dr. \quad (2.20)$$

It is more convenient to multiply G^s and v^l by the average density $\rho(k_F)=2k_F^3/3\pi^2$, by the statistical weight C_J, and by a factor 2 for the exchange term, and to express the final result in MeV. Let $W^s=(4k_F^3/3\pi^2)C_JG^s$ and $W^l=(4k_F^3/3\pi^2)C_Jv^l$ where $C_J=\frac{3}{4}$ for even l and 5/4 for odd l if $k_0<k_F$; otherwise $C_J=1$ for even l. In Table I, W^s, W^l, and d are given as functions of relative momentum k_0. The result shows that the difference between W^R (the reaction matrix without separation) and W^s+W^l decreases as the relative momentum increases, and they are nearly the same above the average relative momentum $\bar{k}_0=(0.3)^{1/2}k_F$.

This same method can be applied in the following way for separating the tensor force. Consider the coupled differential equations

$$d^2\chi(r)/dr^2+f(r)\chi=m^*(-v_c\varphi+V_t\xi), \quad (2.21)$$

$$d^2\xi(r)/dr^2+g(r)\xi=-m^*V_t(\varphi-\chi), \quad (2.22)$$

with

$$f(r)=-(\gamma^2+m^*v_c)$$

and

$$g(r)=-[\gamma^2+6/r^2+m^*(v_c-V_t/\sqrt{2}-3v_{LS}-3v_{LL})],$$

where $\chi=\varphi-u_0$ and $\xi=-u_2$, u_0 and u_2 are perturbed wave functions, and $V_t=(8)^{1/2}v_t$. At $r=c$, vanishing of the wave functions implies that

$$\chi(c)=\varphi(c), \quad (2.23a)$$

and

$$\xi(c)=0. \quad (2.23b)$$

We factorize (2.21) and (2.22) into the following six first-order differential equations:

$$dY_1/dr=-[1+f(r)Y_1^2], \quad (2.24)$$

$$dY_2/dr=-Y_1[f(r)Y_2+m^*(v_c\varphi-V_t\xi)], \quad (2.25)$$

$$dY_3/dr=f(r)[Y_3Y_1+Y_2]+m^*(v_c\varphi-V_t\xi), \quad (2.26)$$

$$dZ_1/dr=-[1+g(r)Z_1^2], \quad (2.27)$$

$$dZ_2/dr=-Z_1[m^*V_t(\varphi-\chi)+g(r)Z_2], \quad (2.28)$$

$$dZ_3/dr=g(r)[Z_3Z_1+Z_2]+m^*V_t(\varphi-\chi). \quad (2.29)$$

Here

$$\chi=Y_1Y_3+Y_2, \quad (2.30)$$

and

$$\xi=Z_1Z_3+Z_2. \quad (2.31)$$

If d is the separation distance, $\chi(d)=\chi'(d)=0$ as before, and for $r>d$ we put $v_c=V_t=0$. We can then solve (2.22), with the result that $\xi=Crh_2^{(1)}(i\gamma r)$, $r>d$, where $h_2^{(1)}$ is the spherical Hankel function of the first kind. Assuming the continuity of ξ at $r=d$, we have

$$\frac{\xi'(d)}{\xi(d)}=\left[\frac{d(rh_2^{(1)})}{dr}\Big/(rh_2^{(1)})\right]_{r=d}. \quad (2.32)$$

Now there are five boundary conditions (2.23a,b), (2.6a,b), and (2.32), four of them for the system (2.24)–(2.29) and one for determination of d. To start integration we need to know ξ and for this we use $\xi=A[e^{-\alpha(r-c)}-e^{-\beta(r-c)}]$ with parameters A, α, and β adjusted so that $(-\xi)$ represents the D wave of the deuteron, we integrate (2.24), (2.25), and (2.26) in exactly the same way as we did for Eqs. (2.7), (2.8), and (2.9); then from (2.30) we calculate χ. Knowing χ we are able to integrate the equations for Z_1 and Z_2 from c to d. From Eqs. (2.27), (2.28), (2.29), (2.31), and (2.32) it follows that

$$Z_3(d)=-\left[Z_2(d)\left(\frac{d(rh_2^{(1)})}{dr}\right)_{r=d}\right]\Big/\left[rh_2^{(1)}+Z_1(r)\left(\frac{d(rh_2^{(1)})}{dr}\right)\right]_{r=d}. \quad (2.33)$$

With this value of Z_3 we can integrate (2.29) from d to c and find ξ from (2.31). Usually two or three iterations are enough to give an accurate value of d, χ, and ξ. In Table II, the separation distance, the contribution of the short- and the long-range parts, and the complete reaction matrix W^R are given for the ^3S state. Unlike the ^1S state, here the difference between the sum of the leading terms in the separation method and W^R is large. This is due to the fact that the tensor force is strong and has a long tail, so that higher order terms are not small, and although the separation distance is reasonable yet this scheme is not very useful, at least for the potentials with a strong tensor force. It is interesting to note that the magnitude of the separation distance d is reasonable both for ^1S and ^3S (although somewhat larger than that obtained by Moszkowski and Scott,[9]) and that it does not depend strongly on k_0. In Fig. 1 we have shown $d(k_0)$ vs k_0 for ^1S and ^3S states.

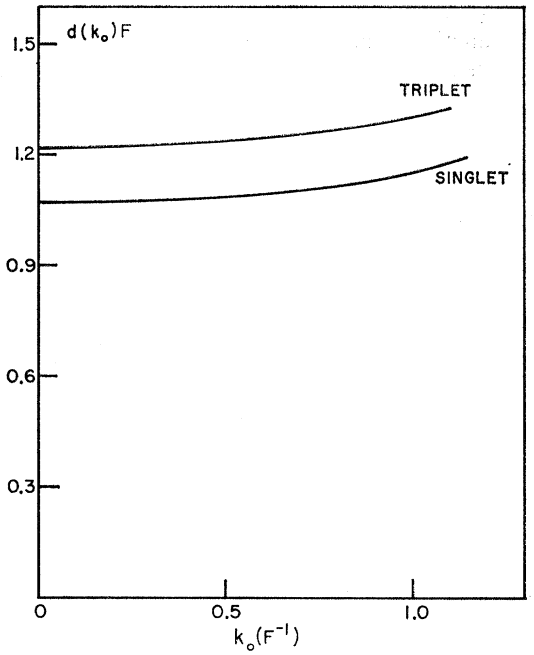

FIG. 1. Separation distance d as a function of relative momentum k_0 in ^1S and ^3S states with $m^*=0.8$ and $\Delta=0.75$.

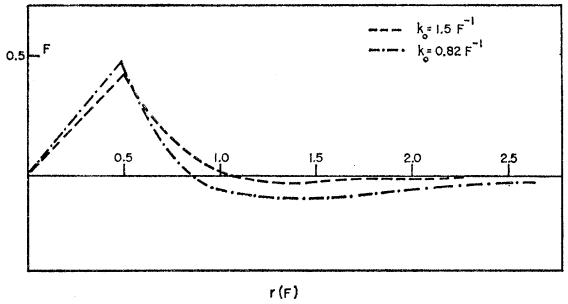

FIG. 2. The difference wave function $\chi=\varphi-r\psi$ for the ^1S state for $k_0=(0.3)^{1/2}k_F$ and k_F, $k_F=1.5$ F^{-1}.

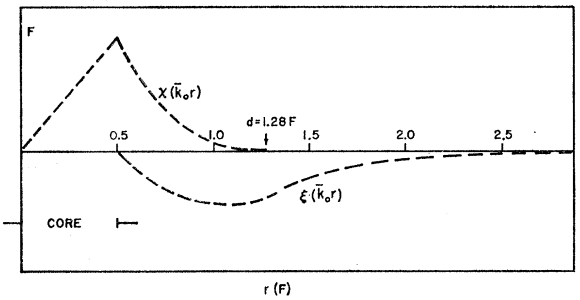

FIG. 3. χ and ξ, the solutions of Eqs. (2.21) and (2.22), are plotted as functions of r for $\bar{k}_0=0.821$ F^{-1}. d is the separation distance.

III. CALCULATION OF G^R

We modify our method of solving (2.5) for the short-range part of the reaction matrix in order to apply it to the differential equation (2.1) with boundary conditions (2.3) and (2.4). If we choose d large enough so that $v(r>d)$ becomes negligible, then for a fixed $r=d$, the boundary condition (2.6) can be replaced by

$$\frac{\chi'(d)}{\chi(d)}=\left[\frac{d[rh_l^{(1)}(i\gamma r)]/dr}{rh_l^{(1)}(i\gamma r)}\right]_{r=d}, \tag{3.1}$$

which determines $Y_3(d)$:

$$Y_3(d)=-\left[\frac{\{d[rh_l^{(1)}(i\gamma r)]/dr\}Y_2}{\{d[rh_l^{(1)}(i\gamma r)]/dr\}Y_1+rh_l^{(1)}(i\gamma r)}\right]_{r=d}. \tag{3.2}$$

Similarly for coupled states we have four boundary conditions (2.23a,b), (2.33), and (3.2). In the numerical calculation $d=10$ F has been used. For $l>2$, nearly all of the contribution to G^R comes from the one-pion exchange potential (OPEP) part of the potential. We extend this part of the potential all the way to the origin. This will not change the results appreciably since $rj_{l>2}(k_0r)$ is very small in the range $0<r<c$. The v_{LL} part of the potential has a long range, but since its existence for the high-energy regions ($k\sim 2k_F$) in which we are interested is doubtful, we neglect it completely. The statistical average for the diagonal elements of G^R for all values of l is[11]

$$\tfrac{1}{16}\sum_{S,M,T,T_3}\langle\varphi_{S,T^M}|G^R|\varphi_{S,T^M}\rangle$$

$$=8\pi\Big[\tfrac{1}{16}\sum_{\text{odd }l}(2l+1)\int_0^\infty rj_lv(S=0,T=0)u_l\,dr+\tfrac{3}{16}\sum_{\text{even }l}(2l+1)\int_0^\infty rj_lv(S=0,T=1)u_l\,dr$$

$$+\tfrac{1}{16}\sum_{\text{even }l,l'}\sum_J(2J+1)\int_0^\infty rj_lv_{l,l'}{}^{(J)}(S=1,T=0)u_{l',J}{}^{(l)}\,dr+\tfrac{3}{16}\sum_{\text{odd }l,l'}\sum_J(2J+1)$$

$$\times\int_0^\infty rj_lv_{l,l'}{}^{(J)}(S=1,T=1)u_{l',J}{}^{(l)}\,dr\Big]. \tag{3.3}$$

TABLE II. The leading terms of the reaction matrix in the ^3S state for different relative momenta. W^R is the reaction matrix for the complete potential. $k_F=1.5$ F^{-1}.

k_0/k_F		0	$(0.1)^{1/2}$	$(0.2)^{1/2}$	$(0.3)^{1/2}$
$d(k_0)$	(F)	1.22	1.24	1.26	1.28
W^s	(MeV)	19.7	19.6	19.4	19.4
$W_c{}^l$	(MeV)	−37.4	−23.4	−15.9	−11.4
$2\rho C_J\left\langle k_0\left\vert V_t{}^l-V_t{}^l\frac{1}{e^R}\right\vert k_0\right\rangle$		−15.1	−11.3	−8.7	−6.6
Sum	(MeV)	−32.8	−15.1	−5.2	1.4
W^R	(MeV)	−50.4	−26.5	−13.2	−6.2

[11] See reference 1(a), Eq. (6.14a).

It is well known that because of the centripetal barrier the presence of the potential will not deform the wave function from the unperturbed one by an appreciable amount, i.e., $u_{l>2}(k_0r)\sim rj_{l>2}(k_0r)$. In other words, the Born approximation, which for these partial waves is the same as the phase-shift approximation, is valid. Taking $u_l=rj_l=u_{l',J}{}^{(l)}$ we can carry out the summation over J in $v_{l,l'}{}^{(J)}$, and this will eliminate v_{LS} and v_t leaving just the central potential (we have already neglected v_{LL}). Now the only summation left is over l. From this we subtract corresponding values of $l=0$, 1, and 2 to get:

$$\tfrac{1}{16}\sum_{S,M,T,T_3}\langle\varphi_{S,T}{}^{M}|G^R|\varphi_{S,T}{}^{M}\rangle$$

$$=8\pi\Big[\tfrac{1}{16}\sum_{\text{odd }l>2}(2l+1)\int_0^\infty j_l{}^2(k_0r)v_{\text{OPEP}}{}^c(S=0,\,T=0)r^2dr+\tfrac{3}{16}\sum_{\text{even }l>2}(2l+1)\int_0^\infty j_l{}^2(k_0r)v_{\text{OPEP}}{}^c(S=0,\,T=1)$$

$$\times r^2dr+\tfrac{3}{16}\sum_{\text{even }l>2}(2l+1)\int_0^\infty j_l{}^2(k_0r)v_{\text{OPEP}}{}^c(S=1,\,T=0)r^2dr+\tfrac{9}{16}\sum_{\text{odd }l>2}(2l+1)$$

$$\times\int_0^\infty j_l{}^2(k_0r)v_{\text{OPEP}}{}^c(S=1,\,T=1)r^2dr\Big]=3\pi V_0[\alpha(\mu,k_0)-\beta(\mu,k_0)],\quad(3.4)$$

where α gives the contribution of the even and β of the odd$l$ states:

$$\alpha(\mu,k_0)=\frac{1}{2\mu^3}+\frac{1}{2\mu(\mu^2+4k_0{}^2)}-\frac{1}{4k_0{}^2\mu}\left\{\left[\frac{15}{2}\left(1+\frac{\mu^2}{2k_0{}^2}\right)-\tfrac{3}{2}\right]\ln\left(1+\frac{4k_0{}^2}{\mu^2}\right)-15\left(1+\frac{\mu^2}{4k_0{}^2}\right)\right\},\quad(3.5)$$

$$\beta(\mu,k_0)=\frac{1}{2\mu^3}-\frac{1}{2\mu(\mu^2+4k_0{}^2)}-\frac{1}{4k_0{}^2\mu}\left[\left(1+\frac{\mu^2}{2k_0{}^2}\right)\ln\left(1+\frac{4k_0{}^2}{\mu^2}\right)-2\right].\quad(3.6)$$

$V_{\text{OPEP}}=V_0e^{-\mu r}/\mu r$, V_0 is the strength, and μ is the range of OPEP. W for $k_0<k_F$ is given by

$$\sum_{l>2}W_l=\frac{2k_F{}^3}{\pi}V_0(\alpha-\beta).\quad(3.7)$$

If $k_0>k_F$, we sum over the even angular momenta only,[12] and the statistical factor C_J will be 1 instead of $\frac{3}{4}$. Hence

$$\sum_{l>2}W_l(k_0)=(8k_F{}^3/3\pi)V_0\alpha.\quad(3.8)$$

In Table III, values of $W(k_0)$ for average relative momentum $\bar{k}_0=(0.3)^{1/2}k_F$, and for different states are given. These results are obtained with the reference spectrum parameters $m^*=1-0.1(k_F/1.5)^3$ (k_F in units

TABLE III. Contribution of different waves to W^R for the average relative momentum $\bar{k}_0=(0.3)^{1/2}k_F$. Only the ^1S contribution has been calculated by the separation method. All unmarked units are in MeV.

k_F (F^{-1})	1.1	1.3	1.5
$\bar{k}_0$ (F^{-1})	0.602	0.712	0.821
$^1S_0$	−13.1	−15.7	−15
$^3S_1$	−28.7	−30.7	−25.7
$^1P_1$	3.4	6.	10.2
$^3P_0$	−4.4	−7	−9.6
$^3P_1$	9.9	18.1	30.2
$^3P_2$	−5.5	−11.2	−20
$^1D_2$	−2.3	−4.9	−9.2
$^3D_3$	−0.1	−0.3	−0.6
$^3D_1$	1.4	3.	5.5
$^3D_2$	−3.7	−7.7	−13.8
$\sum_{l>2}W_l$	1.1	2.2	4.1

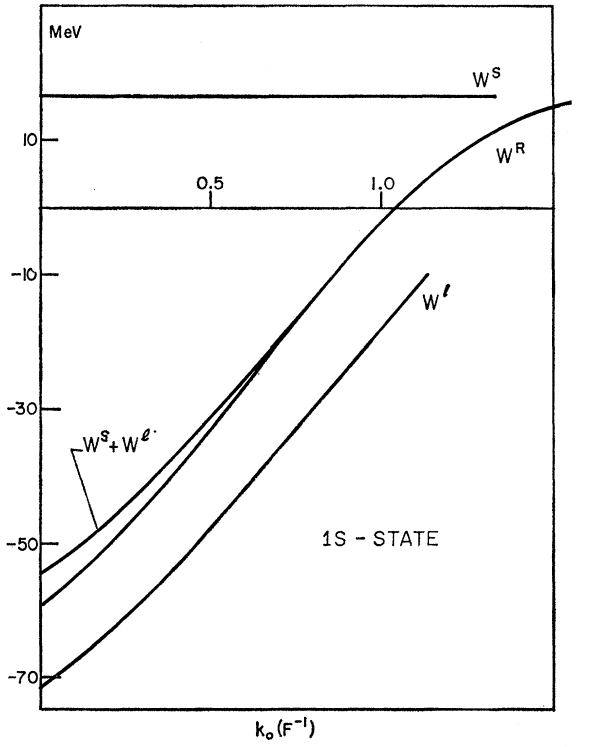

FIG. 4. Diagonal elements of G^R for ^1S as a function of k_0. W^s and W^l are proportional to the short- and the long-range parts of the reaction matrix.

[12] See reference 1(b), Sec. 5.

of F^{-1}) and $\Delta=0.6$. Figures 4, 5, 6, and 7 show $W(k_0)$ as function of k_0 for different waves. For comparison the results of using the separation method for ^1S and ^3S are shown in Figs. 4 and 5. Note that for the computation of these numbers we have used $m^*=0.8$, $\Delta=0.75$, and $k_F=1.5$ F^{-1}.

It is interesting to compare the relative magnitude of the various contributions to the reaction matrix (Table III). The ^3S state gives a much larger contribution than ^1S, in spite of the fact that the tensor force tends to decrease ^3S. Each of the ^3P states gives substantial contribution, but the sum of the contribution is always zero for all values of k_F. On the other hand, the D states give a strong negative contribution, while the sum of the contributions of all other states ($l>2$) is small and positive.

The variation of (W^s and W_l) for the ^1S and W^R for the ^3S as functions of k_F show that both of these states saturate, but because of the tensor force effect the ^3S saturates at a lower density than ^1S. On the contrary W^R for P and D waves tend to increase with k_F (Figs. 4 and 5).

IV. THE PARTICLE ENERGIES

Our detailed calculation with $\Delta=0.75$, $m^*=0.8$, and $k_F=1.5$ F^{-1} shows that $W_m(k_0)=\sum_{l=0}^{\infty} W_l(k_0)$ can be well fitted with

$$W_m(k_0)=B+C/(D^2+k_0^2), \tag{4.1}$$

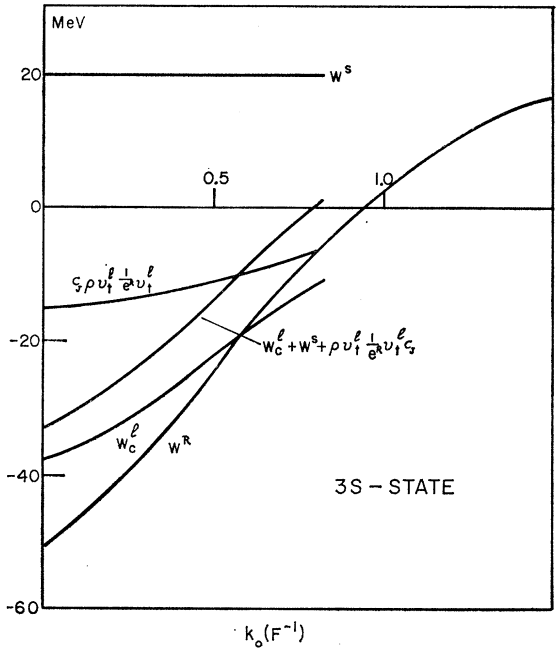

FIG. 5. The leading terms of the reaction matrix for the separation method in the ^3S state. Since $\xi(r>d)\neq 0$ the additional term $C_J\rho v_t^l(1/e^R)v_t^l$ should be added to W_c^s and W_t^s. W^R for this state is also shown.

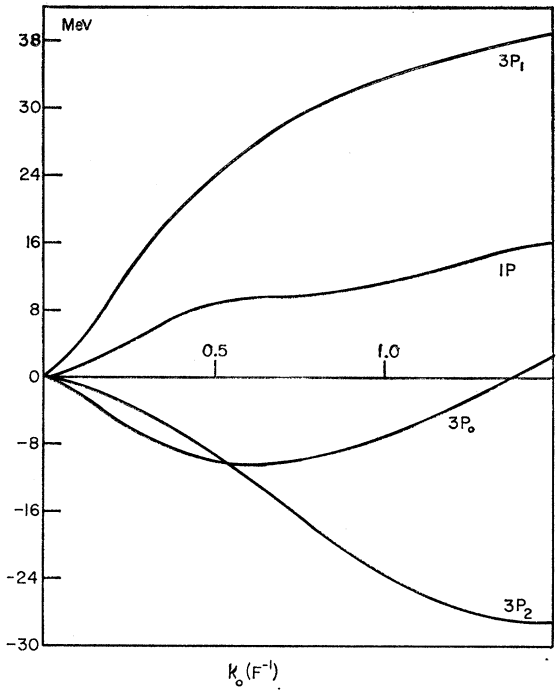

FIG. 6. Diagonal elements of W^R for P waves.

where B, C, and D are constants. (We use subscript m for particles in the Fermi sea and b for particles in the intermediate states.) We assume that the same function with different constants can also fit $k_F=1.1$, 1.3, and 1.5 F^{-1} with different Δ and m^* values. To find B, C, and D we need to know $W_m(k_0)$ for three values of k_0, for which we choose $k_0/k_F=0$, $(0.3)^{1/2}$, 1. For relative momenta $k_0>k_F$, W_b is a quadratic function of k_0.

$$W_b(k_0)=\sum_l W_l(k_0)=A'+B'k_0^2, \quad k_0>k_F. \tag{4.2}$$

This is strictly true only for large values of k_0, so that W_b may have a different dependence on k_0 for $k_0\sim k_F$. Since we have calculated $W_b(k_0)$ for only two points, ($k_0/k_F=1.5$, 2), we will still use (4.2), but more accurate

TABLE IV. Various constants defined by Eqs. (4.1) and (4.2).

k_F (F^{-1})	1.1	1.3	1.5
A' (MeV)	−20.1	6.7	45.3
B' (MeV F^2)	10.4	9.7	11
B (MeV)	−6.5	11	45.3
C (MeV F^{-2})	−30.3	−65.9	−124.2
D (F^{-1})	0.7	0.78	0.85

calculation is needed for the determination of the exact shape of $W_b(k_0)$. Numerical values of B, C, D, A', and B' are given in Table IV. The single-particle potential energy $U(k_m)$ can be obtained from $W_m(k_0)$ by first substituting $k_0=\frac{1}{2}(\mathbf{k}_m-\mathbf{k}_n)$ in (4.1), then integrating over the coordinates of k_n, and finally to preserve the normalization of $W_m(k_0)$, dividing the result by $\int d\mathbf{k}_n$.

$$U(k_m)=\int\left[B+\frac{4C}{4D^2+(\mathbf{k}_m-\mathbf{k}_n)^2}\right]d\mathbf{k}_n\Big/\int d\mathbf{k}_n=B+\frac{3C}{k_mk_n}\left\{\left(\tfrac{1}{2}-\frac{k_m^2}{2k_F^2}+\frac{2D^2}{k_F^2}\right)\ln\frac{4D^2+(k_m+k_F)^2}{4D^2+(k_m-k_F)^2}\right.$$
$$\left.+\frac{2k_m}{k_F}-\frac{4k_mD}{k_F^2}\arctan\frac{4k_FD}{4D^2+k_m^2-k_F^2}\right\}. \quad (4.3)$$

The average potential energy per particle $\bar{U}_m$ is defined as $\bar{U}_m=\int U(k_m)d\mathbf{k}_m/\int d\mathbf{k}_m$, however, it is easier to calculate it directly from $W_m(k_0)$. Thus, the potential energy per particle is given by multiplying $W(k_0)$ by the probability of finding a pair of particles with relative momentum between k_0 and k_0+dk_0 and integrating over the range of k_0. Denoting the unnormalized probability distribution of relative momentum by

$$P(k_0)=k_0^2(1-3k_0/2k_F+k_0^3/2k_F^3),$$

then

$$\bar{U}_m=\int_0^{k_F}W_m(k_0)P(k_0)dk_0\Big/\int_0^{k_F}P(k_0)dk_0=B+\frac{24C}{k_F^2}\left[\tfrac{3}{8}-\frac{D}{k_F}\arctan\frac{k_F}{D}-\frac{D^2}{4k_F^2}+\frac{D^2}{4k_F^2}\left(3+\frac{D^2}{k_F^2}\right)\ln\frac{D^2+k_F^2}{D^2}\right]. \quad (4.4)$$

The binding energy per particle $\bar{E}$ is the sum of the average kinetic energy and one-half of the average potential energy

$$\bar{E}=\bar{T}+\tfrac{1}{2}\bar{U}_m=\frac{3}{10}\frac{\hbar^2}{M}k_F^2+\tfrac{1}{2}\bar{U}_m. \quad (4.5)$$

$U(k_b)$ can be calculated in the same way as $U(k_m)$, and since $W_b(k_0)$ is assumed to be a quadratic function of k_0,

$$\int k_0^2d\mathbf{k}_n\Big/\int d\mathbf{k}_n=\int\tfrac{1}{4}(\mathbf{k}_b-\mathbf{k}_n)^2d\mathbf{k}_n\Big/\int d\mathbf{k}_n$$
$$=\tfrac{1}{4}[k_b^2+0.6k_F^2].$$

Hence,

$$U(k_b)=\left(A'+\frac{0.6k_F^2B'}{4}\right)+\frac{B'}{4}k_b^2. \quad (4.6)$$

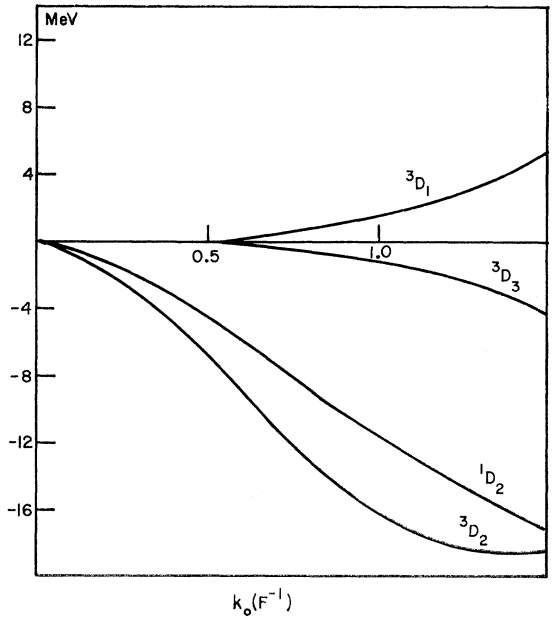

FIG. 7. Diagonal elements of W^R for D waves.

The single-particle energies in the Fermi sea, $E(k_m)$, and above the Fermi sea, $E(k_b)$, are given by

$$E(k_m)=\frac{\hbar^2k_m^2}{2M}+U(k_m) \quad (4.7)$$

and

$$E(k_b)=\frac{\hbar^2k_b^2}{2M}+U(k_b)=\left(A'+\frac{0.6k_F^2B'}{4}\right)+\frac{\hbar^2k_b^2}{2m^*M}, \quad (4.8)$$

respectively, where

$$m^*=\frac{1}{1+B'M/2\hbar^2} \quad (4.9)$$

is the effective mass parameter of the reference spectrum. Similarly, we can find the energy gap Δ which is proportional to the difference of the particle energies in the intermediate state and in the Fermi sea for the average momentum $\bar{k}_b=\bar{k}_m=(0.6)^{1/2}k_F$, i.e.,

$$\Delta=\frac{m^*M}{\hbar^2k_F^2}[E(\bar{k}_b)-E(\bar{k}_m)]$$
$$=\frac{m^*M}{\hbar^2k_F^2}[U(k_b)-U(k_m)]. \quad (4.10)$$

The self-consistency may be checked by evaluating Δ and m^* from (4.9) and (4.10) and comparing it to the values which were assumed at the beginning. Numerical results for $\bar{U}_m$, $\bar{E}$, and $U(k_m)$ are given in Table V and for Δ and m^* in Table VI.

TABLE V. Single-particle potential energies and the binding energy $\bar{E}$. All unmarked units are in MeV.

k_F (F^{-1})	1.1	1.3	1.5
$\bar{U}_m$	−44.8	−54.5	−55.4
$\bar{E}$	−7.4	−6.2	0.31
$U(k_m=0)$	−52.6	−66.8	−74.7
$U(\bar{k}_m)$	−44.7	−52.8	−51.5
$U(k_m=k_F)$	−40.9	−45.8	−40.6
$E(k_m=k_F)$	−15.9	−10.8	5.9

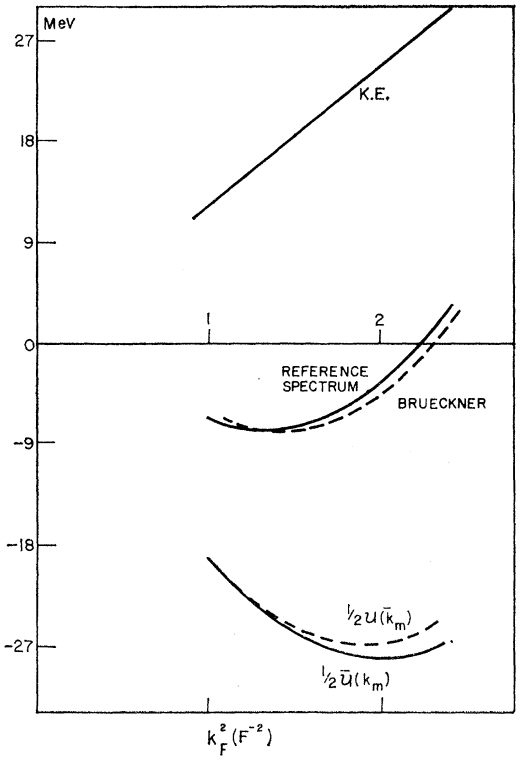

FIG. 8. The average single particle potential energy $\bar{U}(k_m)$, the single particle potential energy for average momentum $U(\bar{k}_m)$, and binding energy per particle $\bar{E}$, is shown as a function of k_F^2. For comparison we have also plotted Brueckner's results for the Breit potential.

V. DISCUSSION

Our separation method in ^1S is satisfactory, while in ^3S, because of the cancellation between rather large W^s and W^l, we have a small first-order term. The tensor contribution comes mainly in the form[9] $v_t{}^l(Q/e^N)v_t{}^l$ and this is much larger than $v_c{}^l(Q/e^N)v_c{}^l$; for this reason the convergence of the series is not fast. We have considered an alternative method of separating the potential in the S wave only, leaving the whole potential to act in the D wave, in this way increasing the first-order terms. However, higher order terms are difficult to calculate for the reason that the operators are no longer Hermitian. Besides devising a better method of separation for the tensor force, one can think of other important improvements on the present calculation. The following are some of the important changes that should be made in a more accurate computation. (1) To make the second-order terms as small as possible, it seems that instead of using a Δ independent of k_F, one should allow for its dependence on k_F as our results suggest. These indicate that Δ increases with k_F, but they do not clearly show the variation of m^* with k_F. This is due to the form of $W_b(k_0)$, and it is doubtful that the quadratic form of (4.2) is a good approximation, especially for $k_0 \sim k_F$. It should be pointed out that m^* is nearly 1, and its exact value is not very important. Therefore, it is also unimportant how m^* varies with k_F. However, to obtain the spectral correction it would be necessary to get accurate values of U_b for smaller k_F. (2) The work of Rajaraman shows that for the states outside the Fermi sea, to calculate U_b one should consider even states only with the statistical factor equal to one (as we have calculated U_b here). This has been proved for spin-independent, isotropic interactions, however tensor forces may give a somewhat different result. In this calculation tensor forces have been treated in the same way as the central forces. (3) Another factor which should be treated more consistently is the v_{LL} part of the potential. While we have included it in evaluating G^R for S, P, and D waves we have neglected it for higher partial waves. Although this force is not very important for small k_0, it plays an important role in the states above the Fermi sea. Thus, it is an important factor in the determination of Δ and m^*.

TABLE VI. Reference spectrum parameters. Subscript i refers to the initial and f to the final values. The final values of Δ indicate a strong dependence on k_F, and the difference between Δ_f and Δ_i is large for $k_F = 1.5$ F^{-1}.

k_F (F^{-1})	1.1	1.3	1.5
m_i^*	0.96	0.935	0.9
Δ_i	0.6	0.6	0.6
m_f^*	0.89	0.90	0.88
Δ_f	0.46	0.71	0.95

The first-order terms (i.e., the reaction matrix for the reference spectrum without Pauli and the spectral corrections) as we have calculated here show saturation with an energy minimum $\bar{E} = -7.8$ MeV at a Fermi momentum $k_F = 1.12$ F^{-1}, which corresponds to an equilibrium spacing $r_0 = 1.35$ F. For $k_F = 1.5$ F^{-1} we do not get a bound system, rather $\bar{E} = 0.3$ MeV, if we include all partial waves; however, if we take just the even states, i.e., S and D waves, then $\bar{E} = -6.3$ MeV. It should be pointed out that the difference between Δ_i and Δ_f (subscript i for initial and f for final values) is largest for $k_F = 1.5$ F^{-1} (Table VI). Therefore, correction terms here are more important than for $k_F = 1.1$ and 1.3 F^{-1}. The second-order terms would change the above results by 2 or 3 MeV.

Rather similar results are reported by Brueckner and Masterson. They found that for the Breit potential the minimum energy is $\bar{E} = -8.3$ MeV at $r_0 = 1.28$ F, while at $k_F = 1.52$ F^{-1} they obtained a very small binding of -0.3 MeV for all partial waves, and -9.2 MeV for S and D waves alone. Although Brueckner's formalism is different from ours, and the potentials used are not exactly the same, yet it would be difficult to believe that the similarity between these calculations is purely accidental. Moreover, Blatt *et al.*,[13] have calculated the

[13] J. M. Blatt, G. H. Derrick and J. N. Lyness, Phys. Rev. Letters 8, 323 (1962).

TABLE VII. Parameters of Hamada-Johnson potential as defined in the Appendix.

State	a_c	b_c	a_t	b_t	G_{LS}	b_{LS}	G_{LL}	a_{LL}	b_{LL}
Singlet even	+8.7	10.6	···	···	···	···	−0.000891	+0.2	−0.2
Triplet odd	−9.07	+3.48	−1.29	+0.55	+0.1961	−7.12	−0.000891	−7.26	+6.92
Triplet even	+6.0	−1.0	−0.5	+0.2	+0.0743	−0.1	+0.00267	+1.8	−0.4
Singlet odd	−8.0	+12.0	···	···	···	···	−0.00267	+2.0	+6.0

binding energy of the triton, using both the Hamada-Johnson and Breit potentials. They have found similar results for both potentials, namely, −2.6 MeV for the first and −2.5 MeV for the second. These values are, of course, much higher than the experimental value of −8.49 MeV.

In the Hamada-Johnson potential we have the following features which, according to Brueckner, are responsible for the low equilibrium density and the small binding energy: (a) larger core radius, (b) strong odd-state repulsion, (c) quadratic spin-orbit terms, and (d) weaker even-triplet central force. As Brueckner has pointed out, the results of all these calculations indicate the need for further studies on the nature of nucleon-nucleon interactions.

ACKNOWLEDGMENTS

The author wishes to thank Professor H. A. Bethe for suggesting this problem and for his continued guidance and interest in this work. He is also grateful to E. J. Irwin and B. H. Brandow for many helpful discussions, and to the Cornell Computing Center for the use of computing facilities.

APPENDIX

The Hamada-Johnson potential is of the form

$$v=v_c+v_tS_{12}+v_{LS}(\mathbf{L}\cdot\mathbf{S})+v_{LL}L_{12},$$

where c, t, LS, and LL, refer to central, tensor, linear $\mathbf{L}\cdot\mathbf{S}$ and quadratic $\mathbf{L}\cdot\mathbf{S}$ potentials, respectively. L_{12} is the operator defined by

$$L_{12}=\delta_{LJ}+(\boldsymbol{\sigma}_1\cdot\boldsymbol{\sigma}_2)\mathbf{L}^2-(\mathbf{L}\cdot\mathbf{S})^2.$$

v_c, v_t, v_{LS}, and v_{LL} are given by

$$v_c=0.08(\mu/3)(\boldsymbol{\tau}_1\cdot\boldsymbol{\tau}_2)(\boldsymbol{\sigma}_1\cdot\boldsymbol{\sigma}_2)Y(x)[1+a_cY(x)+b_cY^2(x)].$$

$$v_t=0.08(\mu/3)(\boldsymbol{\tau}_1\cdot\boldsymbol{\tau}_2)(\boldsymbol{\sigma}_1\cdot\boldsymbol{\sigma}_2)Z(x)[1+a_tY(x)+b_tY^2(x)],$$

$$v_{LS}=\mu G_{LS}Y^2(x)[1+b_{LS}Y(x)],$$

and

$$v_{LL}=\mu G_{LL}x^{-2}Z(x)[1+a_{LL}Y(x)+b_{LL}Y^2(x)].$$

Here μ is the pion mass ($\mu=139.4$ MeV), x is measured in μ^{-1}, $Y(x)=e^{-x}/x$, and $Z(x)=(1+3/x+3/x^2)Y(x)$. For numerical values of the parameters used in these potentials see Table VII. The hard-core radius is $c\mu=0.343$ in all states.